Asian Journal of Green Chemistry 6 (2022) 175-184

Asian Journal of Green Chemistry

Journal homepage: www.ajgreenchem.com

Original Research Article

Improving the morphology and electro-optic properties of ITO thin film, by changing argon rate and atmosphere pressure

Mohammad Reza Zamani Meymian[a,*], Mohsen Moradi Haji Jafan[b], Mahboubeh Rabbani[c], Mahdi Behboudnia[b]

[a] *Department of Physics, Iran University of Science and Technology, Tehran, Iran*

[b] *Department of Physics, Urmia University of Technology, Urmia, West Azerbaijan Province, Iran*

[c] *Department of Chemistry, Iran University of Science and Technology, Narmak, Tehran, Iran*

ARTICLE INFORMATION

Received: 11 June 2022
Received in revised: 11 July 2022
Accepted: 12 July 2022
Available online: 21 July 2022

DOI: 10.22034/ajgc.2022.2.7

KEYWORDS

Tin-doped indium oxide
ITO
Sol-gel spin coating
Argon atmosphere
Pressure

ABSTRACT

In this research study, we report the characteristics of Sn-doped In_2O_3 (ITO) films intended for use as transparent conducting electrodes. The ITO thin films were deposited using spin coating method in the frame of a sol-gel process in the presence of polyvinyl alcohol (PVA) as a binder. After using the sol-gel spin coating method, Indium tin oxide thin films were annealed at 550 °C under different argon rates (from 50 to 150 mL/min) and pressures (from 10 to 650 torr) for 45 min. The influence of different rates of argon pressure on the microstructure, and electrical and optical properties of ITO surfaces were evaluated using XRD, EDX, SEM, UV–Vis, and four-point probe. Wettability of the ITO surface was indicated in hydrophobicity with a contact angle (CA) of 0° before annealing. XRD patterns illustrated that all the films are polycrystalline of Cbb structure with preferentially oriented along (222) plane. The SEM images showed that the grain size of ITO nanoparticles and the thickness of the films were obtained at about 70-150 nm and 400-450 nm, respectively. The analyses were mainly proven here to highlight the role of the rate of argon atmosphere and pressure on the microstructure and the optical and electrical properties of the films. Increasing argon atmosphere and decreasing pressure increase the conductivity and crystallization of samples. The obtained results indicated that minimum sheet resistance (82 Ω/Square and resistivity and or 3.69×10^4 Ω.cm) were achieved for thin films annealed under pressure of 10 torr and argon rate of 150 mL/min So that its transmission range was above 81% and its band gap about 3.73 eV. This sample has better results than the other samples in different conditions and has the best results compared to similar cheap methods. The process was tested repeatedly in data measurement and manufacturing to ensure its repeatability.

Corresponding authors, email: r_zamani@iust.ac.ir (M.R. Zamani Meymian).
Tel.: +98217322 5893.

Graphical Abstract

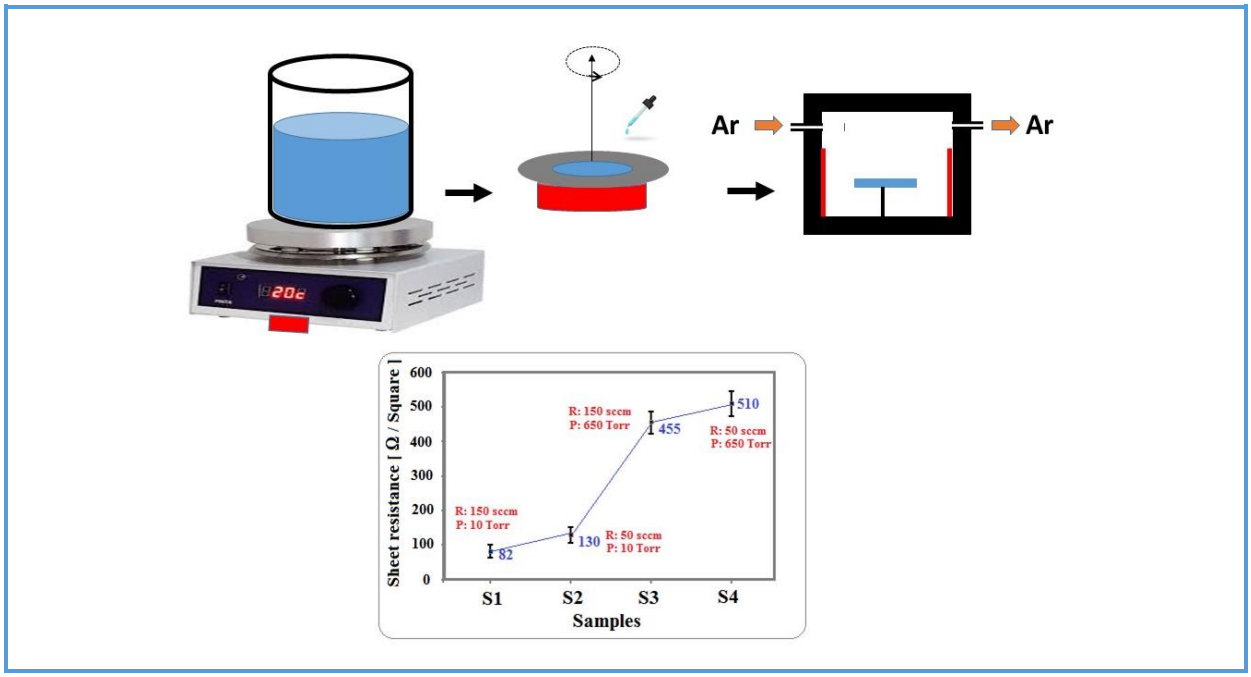

Introduction

Transparent conducting oxides (TCOs) are known materials that play essential roles as transparent electrodes in commercial applications such as solar cells, flat panel displays, and electroluminescent devices as transparent electrodes [1–3]. Among them, indium tin oxide (ITO) films have high electrical conductivity and optical transparency in the visible region [4] and are used as transparent conductive electrodes in virtually every photoelectric device [5]. Various techniques have been used to fabricate ITO thin films, such as evaporation [6–8] and sputtering [9–11]. These methods, which require high temperatures and high vacuum, are expensive to manufacture. Sol–gel-spin coating can be applied to the practical preparation of large area films because of its simplicity, easily doping control, and thickness [12–14]. Today there is a strong need for high-quality ITO films with different deposition conditions such as temperature [15–17], annealing pressure [18–19], and rate of argon gas [20–23].

So far, a lot of research has been conducted to optimizing ITO layers. However, there is no research evidence on the simultaneous effect of argon gas pressure and rate on ITO layers [18–23]. In the present experiment, for the first time, the impact of pressure and rate of argon gas on the microstructure of ITO thin films were studied, and the optical and electrical properties were deeply investigated. The following discussed the relation between conductivity and optical band gap at applied conditions and the ITO surface wettability.

Experimental

Sample preparation

ITO thin films were prepared via sol–the gel spin coating process. For this purpose, the first 1.1 g of Polyvinyl alcohol (PVA, average molecular weight: 65,000, hydrolysis: 85.5–86.5, Dongyang Chem., Korea) as polymerizing

agent and binding material was dissolved in 30 mL of double-distilled water, and the resultant solution was refluxed at 80 °C for 3 h (container A). Next, indium nitrate hydrate ($In(NO_3)_3.H_2O$, Alfa Aesar 99.99%) was dissolved in double-distilled water separately, and the resultant solution (0.5 M) was refluxed at 60 °C for 30 min (container B). Then 0.29 mL (0.25 m mol) of tin chloride anhydrous ($SnCl_4$ Merck 98%) as inorganic reactants (with an initial molar ratio of 9:1 for In:Sn) was dissolved in 5 mL absolute ethanol, and it was stirred for 30 min (container C). Those two obtained solutions (B and C) were separately added to solution A, then mixed and refluxed at 60 °C for another 2 h (pH=2.3) under stirring. Several drops of hydrochloric acid were added to the solution to prevent hydrolysis of $SnCl_4$ during the refluxing until a transparent ITO sol was achieved (pH=1.6). The Sn/In ratio was fixed at 10/90 wt%, respectively. Finally, the obtained sol was aged for 2 days at room temperature.

For the deposition of ITO thin films, glass substrates were washed with a detergent and cleaned ultrasonically with isopropanol, acetone, ethanol, and deionized water for 6 min, respectively. The aged sol was dropped on a glass substrate and then spin-coated by the spin coating technique. Spin parameters, including spin speed and time, were fixed at 2500 rpm and 20 s, respectively. After that, the coated glasses were heated at 150 °C for 20 min to consolidate the layers of indium tin hydroxide. The spinning and drying process were repeated 7 times to reach the favorite film thickness according to our previous work [24]. Eventually, all thin films were annealed at 550 °C at different rates of argon atmospheres (50 and 150 mL/min) and under different pressure (10 and 650 torr) for 1 h. So that the first sample (S1) was annealed under the pressure of 10 torr and at a rate of 150 mL/min, the second sample (S2) was annealed under the pressure of 10 torr and at a rate of 50 mL/min, the third sample (S3) was annealed under the pressure of 650 torr and at a rate of 150 mL/min, the fourth sample (S4) was annealed under the pressure of 650 torr and at a rate of 50 mL/min respectively. Figure 1 illustrates the preparation process of ITO thin films in this study.

ITO thin film's characterization

The crystallinity of the desired thin films was determined by X-ray diffraction using JEOL diffractometer with Cu Ka radiation (λ=1.54 Å). The samples' surface morphology and average thickness were measured using a scanning electron microscope (Tescan Vega II). The elemental composition of ITO samples was determined by energy dispersive X-ray (EDX) analysis. Spectroscopic analysis of the ITO thin films was performed using UV–Vis spectrophotometer (Rayleigh UV-2100) with a wavelength range of 200–900 nm. The resistivity of the thin films was measured by the Jandel resistivity meter (RM3-AR) four aligned probe equipment at 23±2 °C.

Results and Discussions

Figure 2 illustrates the X-ray diffraction patterns of the In_2O_3 doped with SnO_2 thin films prepared at different rate of argon atmospheres and pressure.

All the peaks of samples were analyzed and indexed using JCPDS 06-0416 database and compared with the space group La3 standards. All the Samples illustrate a significant (2 2 2) plan sharp corresponded to a peak at 30.50º, which represents the cubic In_2O_3. , The absence of SnO_2 or other peaks in X-ray diffraction patterns, illustrates that Sn atoms are doped into the In_2O_3 structure. Also, a shift of the (222) peak toward a smaller 2θ value is due to the

replacement of smaller radius Sn^{4+} ion in indium sites [25].

As it can be seen in this Figure 2, when the pressure decreased from 650 to 10 torr, the peaks become sharper with high intensity, which assumes a better crystallization and bigger crystallite size (This result is truthful for both samples at Ar rate). When the Ar rate from 50 mL/min to 150 mL/min, the peaksbecame sharper with high intensity. Of course, the increasing rate of Ar gas compared with its decreasing pressure did not greatly impact crystallite size.

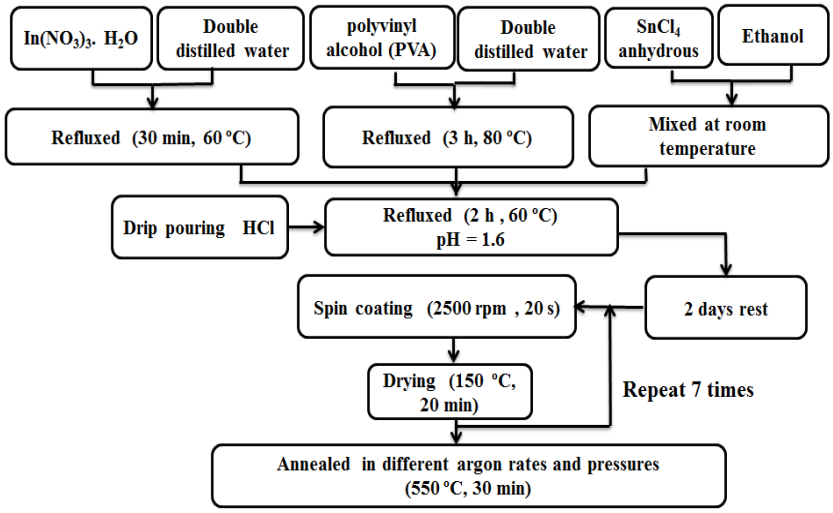

Figure 1. Preparation process of the ITO thin films

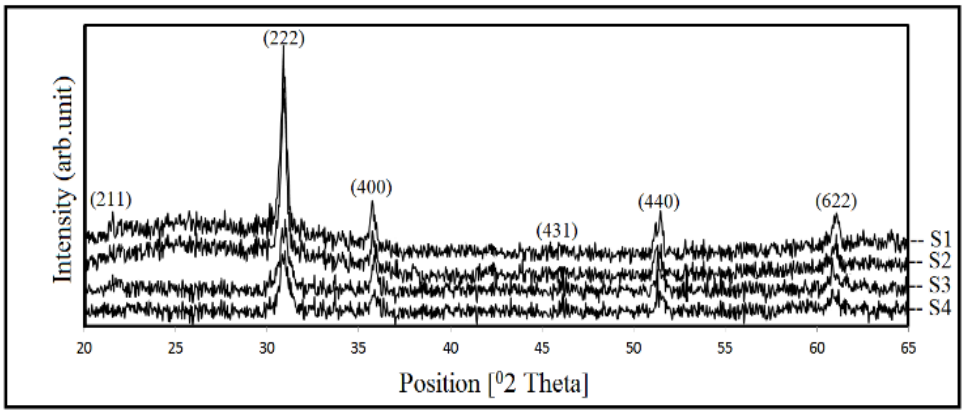

Figure 2. X-ray diffraction patterns of ITO thin films at different condition

The microstructure and surfaces of the samples were evaluated using the scanning electron microscopy. The images of S1, S2, S3, and S4 samples (Figures 3**a-d**) reveal that the films deposited under different conditions have continuous film structure containing uniform nanoclusters due to the presence of polyvinyl alcohol (PVA) as a binder which increases the wettability of the synthesis due to increase of hydroxyl groups. As well as, decomposition of PVA during thermal curing leads to creating an ITO nanocluster [19, 20]. For this purpose, samples S1 and S3 in the 150 mL/min Ar-gas rate, which was annealed at pressures of 10 torr

and 650 torr, respectively, were investigated. As seenin Figure 3, the sample annealed at a pressure of 10 torr (S1) has a larger grain size and is more mesoporous, while the sample annealed at a pressure of 650 torr (S3) has a smaller grain size. To confirm this result, we repeated the experiment under different Ar-gas rates (at a rate of 50 mL/min), see sample S2 (Figure 3**b**) and sample S4 (Figure 3**d**). The sample annealed at a pressure of 10 torr (S2) has a larger grain size and is more mesoporous, while the samples annealed at a pressure of 650 torr (S4) has a smaller grain size. Also, by increasing at Ar-gas rate, the samples tend to get more ordered and spherical. Comparing S1 and S3 with S2 and S4 shows that an increase in the argon rate causes the better growth of ITO thin films, increase in grain size, homogeneity, and surface roughness. In other words, low argon gas rate (S2 and S4) causes a granular structure with small and sharp grain for the deposited samples. The surface morphologies and thickness of ITO thin films were investigated using cross-section scanning electron microscopy. Figure 3**e** shows a cross-section image of one prepared sample (S3). The cross-section SEM images show the thickness of all samples is about 400 to 450 nm, so the electrical resistivity can be obtained. According to our recent research, the molar ratio of tin to indium, 10:90, is the optimum amount that has the best conductivity. As more significant amount of Sn^{4+} ions lead to form Sn_2O_4 compounds, it increases the resistance of the ITO layers [18]. The energy dispersive X-ray analysis (EDX) demonstrates that nearly 10.6% of tin entered into the In_2O_3 sites and is adequate to the content of 10% Sn precursor used to synthesize of ITO (Figure 3**f**).

Figure 4**a** illustrates the optical transmittance spectrum of prepared ITO layers. As shown in this Figure 4, all of the samples have preferable transparency in the visible region (from 370 nm to 750 nm), so the average transmittance of the samples is over 83%. As shown in this Figure, the samples annealed at lower pressures are less transparent, so the samples annealed at 10 torr have average transparency of 78-82% in the wavelength of 400-700 nm, and the reason is the decrease of oxygen in the surface. To compare the samples prepared in the Argon rate of 50 and 150 mL/min, Figure 4 shows that for the samples in which the Ar rate is higher are more transparent than the ones with a lower Ar rate. There is an absorption coefficient for the directly allowed transmittance that can be written by using Tauc's relation:

$$\alpha h\nu = \alpha_0 (h\nu - E_g)^{1/2}$$

Where hν, E_g, and α_o are photon energy, optical band gap, and constant of the ITO thin films, respectively.

The samples' absorption coefficient (α) at different wavelengths can be calculated from the transmission spectra region. Figure 4**b** demonstrates the optical band gap of the ITO layers by drawing $(\alpha h\nu)^2$ per $h\nu$. The diagram shows that all the ITO samples have a band gap between 3.70 eV to 3.88 eV. According to the Figure 4**b**, the sample which is annealed at 10 torr pressure in the rate of 150 mL/min revealed the lowest optical band gap following other samples. When the Ar rate decreases to 50 mL/min, the band gap of the sample increased, and the samples that annealed at 650 Torr pressure at the rate of 150 and 50 mL/min had higher band gaps compared to the previous two samples.

Shapes of water droplets on the prepared ITO thin films before and after annealing is indicated in Figure 5.

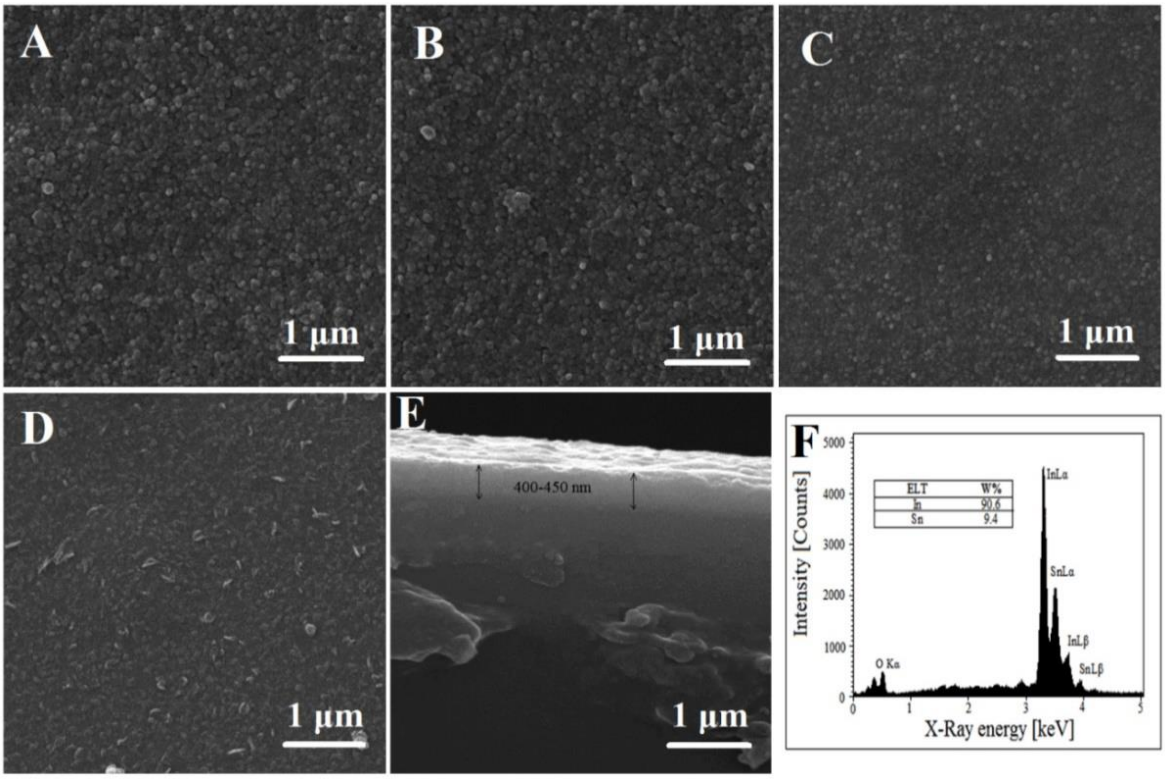

Figure 3. The SEM observation of ITO samples at different conditions: a) S1, b) S2, c) S3 and d) S4. e) the cross-section SEM image of sample (S3), f) the EDX results of sample (S3)

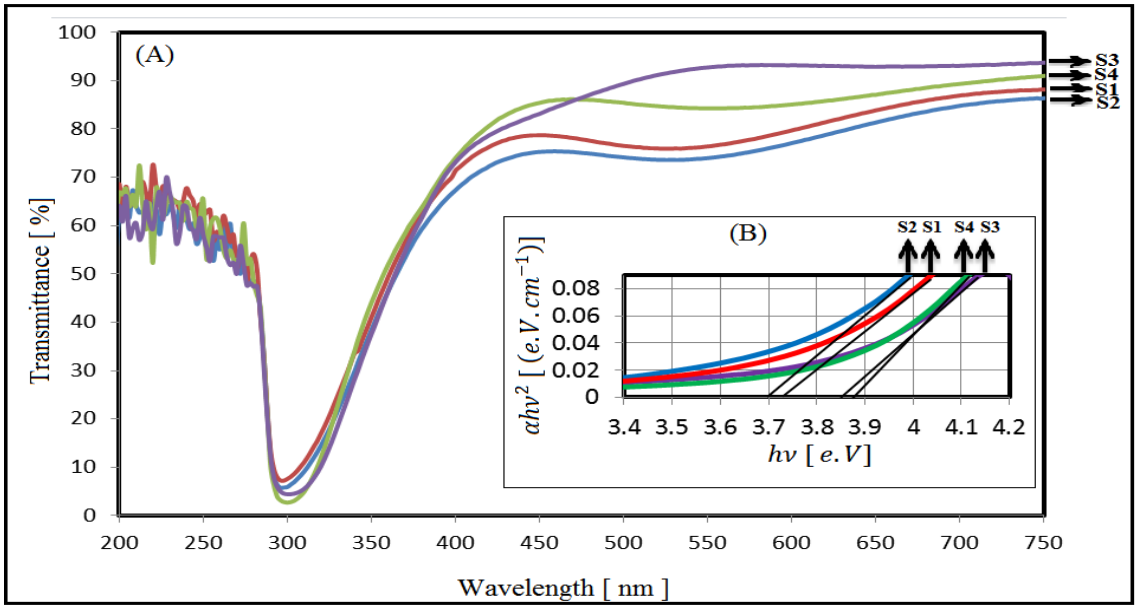

Figure 4. Transmittance spectrum of ITO thin films. Inset: the band gap of ITO samples at different conditions

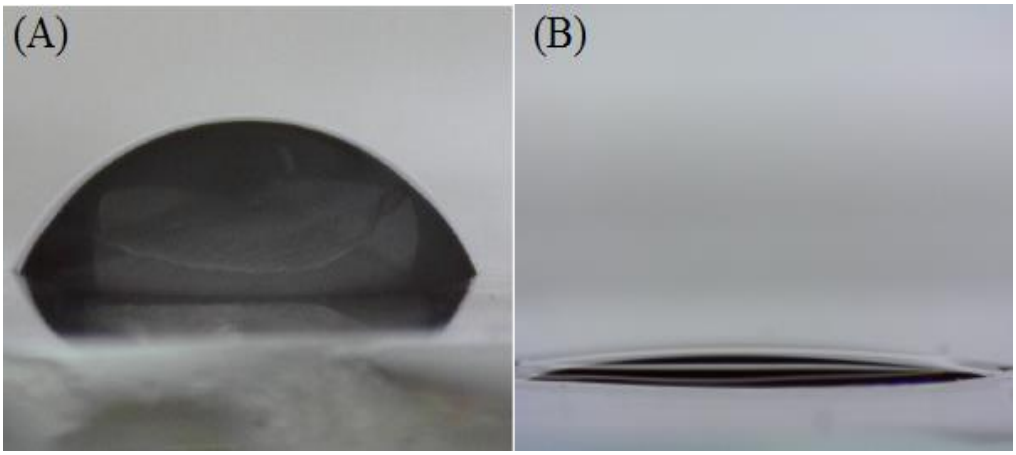

Figure 5. Shapes of water droplets on the prepared ITO thin films a) before and b) after annealing

The electrical resistivity (ρ) of samples was studied using the four-point probe method. According to the results of the four-point probe, R_s, and film thickness obtained by cross-section SEM images, t, and substituting in the following equation, the resistivity of samples can be obtained.

$$\rho = t.R_S \ (\Omega.cm)$$

The prepared samples' average resistivity and sheet resistances in different conditions (pressure and rate of argon gas) are measured and presented in Table 1.

Figure 6 illustrates the conductivity properties of the ITO thin films with the error bar. In ordinary cases the measurement will be reported in the form $\boldsymbol{x \pm u}$ in which x represents the test result, and u represents the uncertainty associated with x. The methodology for uncertainty estimates has been classified as Type A and Type B [26]. In this study, we used type A for measurements. The sheet resistance, R_s, values were obtained from 9 points in a 1×1 cm^2 substrate. As demonstrated, in the same pressure conditions, the samples with higher Ar-gas rate have lower resistivity, which is repeatable. On the other hand, fabrication of the samples in the same argon rate creates lower resistivity by the lower pressures and is repeatable. In other words, when the samples are exposed to atmospheric pressure, the conductivity of the samples decreases on average 4.5 times. When the rate of argon gas increases from 50 to 150 mL/min, the conductivity increases almost 1.5 times.

In those samples, the pressure and rate of argon gas affects the mobility and conductivity of the electron carriers because the creation of the free carriers depends on two mechanisms, including the two-valence oxygen vacancies and the replacement of the four-valenced tin (Sn) ions. An enhancement of the mobility can be because of the improved crystalline structure derived from the increase of the grain sizes and also a higher concentration of the ITO layers [27].

The annealed samples at lower pressure (10 Torr) have the highest conductivity. Figure 7 demonstrates the relation between the electrical condition and the optical band gap of samples. As demonstrated, conduction-band minimum (CBM) is added to the band gap because of the increasing electron carrier's concentration which has increased the optical band gap [25]. As it is seen, sample S3 has better electrical conductivity than sample S4. In contrast, sample S3, which is annealed at 550 °C at 150 mL/min rate of an argon atmosphere, has a larger band gap due to the argon rate. One of

the most significant achievements in this work is the rate of argon atmosphere effect on charge carriers, which leads to an increase in the conduction band. For S1 and S2 samples, the optical band gap decreased by pressure decreasing. This could be due to the improved crystalline structure at lower pressure, which is represented in sizeable crystalline size, and the other factor for decreasing the optical band gap, annealed in lower pressure,Δ_{RN}, that is due to the coulomb interactions of free electrons in the conduction band and electron impurity scattering that guides a decrease in the energy of the conduction-band minimum (CBM) and an increase in the energy of the valence-band maximum (VBM) [25].

Table 1. The effect of annealing pressure and rate of Argon gas on electrical conductivity of various types of samples

Samples	Annealing pressure (Torr)	Rate of Argon gas (mL/min)	Sheet resistance, R_s (Ω/square)	Band gap (eV)	Resistivity, ρ (Ω.cm)
S1	10	150	82±20	3.73	$\sim 3.69 \times 10^4$
S2	10	50	130±23	3.70	$\sim 5.58 \times 10^4$
S3	650	150	455±32	3.85	$\sim 1.82 \times 10^5$
S4	650	50	510±37	3.88	$\sim 2.04 \times 10^5$

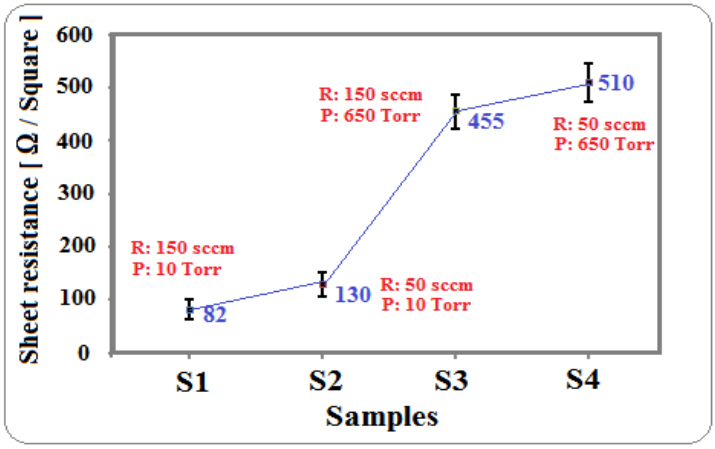

Figure 6. Sheet resistance dependence on different conditions of deposited ITO samples

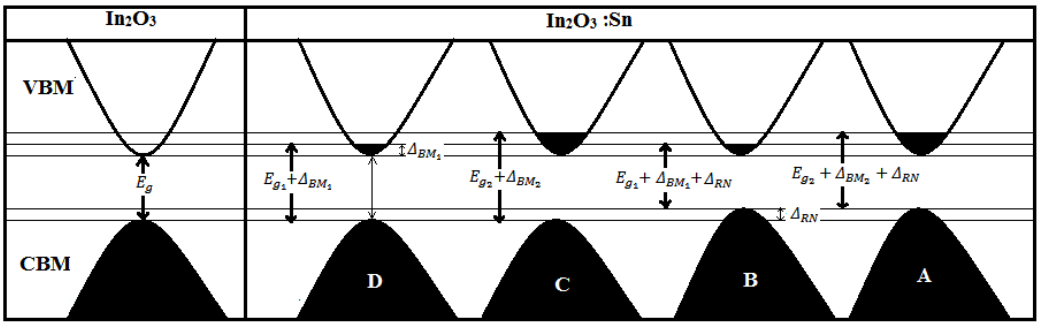

Figure 7. Burstein-Moss effect on optical band gap of ITO thin films

Conclusions

This work has been reported on the fabrication of ITO thin films by adding PVA as a binder. The influence of pressure and argon gas rate on structure, transparency, and resistivity was investigated. Structural investigation showed cubic In_2O_3 with BCC structure for all samples. It was also observed that (2 2 2) primary crystallographic orientation was the preferred orientation for ITO thin film growth with decreasing pressure. The surface morphology of the samples depicted a granular structure with small grains, and the grain size and surface roughness were increased with decreasing pressure and increasing the argon gas flow. It is found that the different pressure and rate of gas have a significant effect on the band gap of samples; as the argon gas rate increases, the band gap increases, and when the pressure decrease, the band gap decreases. The best crystal structure and electrical conductivity belong to the ITO sample, which is first annealed at a pressure of 10 Torr and an argon rate of 150 mL/min (S1) with minimum resistance. Due to changes in pressure and argon rate, the relationship between the electrical conductivity and the optical band gap is studied. Also, it was found that the sample annealed in 10 Torr and argon rate of 50 mL/min (S2) revealed the lowest band gap, 3.70 eV.

Disclosure Statement

No potential conflict of interest was reported by the authors.

References

[1]. Zhang H., Ye F., Liu L., Xu H., Sun C. *J. Alloy. Compd.*, 2010, **504**:171 [Crossref], [Google Scholar], [Publisher]

[2]. Ginley, David S., Hideo Hosono, David C. Paine, eds. *Handbook of transparent conductors*; Springer:New York, 2010, [Crossref], [Publisher]

[3]. Ginle D.S., Perkins J.D. *Transparent conductorsIn Handbook of Transparent Conductors*, 2011, 1 [Crossref], [Publisher]

[4]. Liu Y. *Ludwig-Maximilians-Universität, Diss*, 2012 [Publisher]

[5]. Angmo D., Krebs F.C. *Journal of Applied Polymer Science*, 2013, **129**:1 [Crossref], [Publisher]

[6]. Du J. Chen X.L., Liu C.C., Ni J., Hou G.F., Zhao Y., Zhang X.D. *Applied Physics A.*, 2014, **117**:815 [Crossref], [Google Scholar], [Publisher]

[7]. Ito T., Uchiyama H., Kozuka H. *Langmuir*, 2017, **33**:5314 [Crossref], [Google Scholar], [Publisher]

[8]. Maestre D., de Velasco I.M., Cremades A., Amati M., Piqueras J. *The Journal of Physical Chemistry C.*, 2010, **114:**11748 [Crossref], [Publisher]

[9]. Gulen M., Lee K.M. *Journal of Materials Science: Materials in Electronics*, 2013, **24**:467 [Crossref], [Google Scholar], [Publisher]

[10]. Chen, A., Zhu K., Zhong H., Shao Q., Ge G. *Solar Energy Materials and Solar Cells*, 2014, **120**:157 [Crossref], [Google Scholar], [Publisher]

[11]. Xian Z., Han B., Li S., Yang C., Wu S., Lu X., Gao X., Zeng M., Wang Q., Bai P., Naughton M.J., Zhou G., Liu J.M., Kempa K., Gao J. *Advanced Materials Technologies*, 2017, **2**:1700061 [Crossref], [Google Scholar], [Publisher]

[12]. Duta M., Calderon-Moreno J.M., Predoana L., Preda S., Nicolescu M., Stroescu H., Bratan V., Dascalu I., Aperathitis E., Modreanu M., Zaharescu M., Gartner M. *Journal of Materials Science: Materials in Electronics*, 2016, **27**:4913 [Crossref], [Google Scholar], [Publisher]

[13]. Moradi-Haji J.M., Zamani-Meymian M.R., Rahimi R., Rabbani M. *Journal of Nanostructure*

in Chemistry, 2014, **4:**1 [Crossref], [Google Scholar], [Publisher]
[14]. Park S., Kima C.H., Leea W.J., Sung S., Yoon M.H. *Materials Science and Engineering: R: Reports,* 2017, **114**:1 [Crossref], [Google Scholar], [Publisher]
[15]. Cho H., Yun Y. *Ceramics International*, 2011, **37:**615 [Crossref], [Google Scholar], [Publisher]
[16]. Koseoglu H., Koseoglu H., Turkoglu F., Kurt M., Yaman M.D., Akca F.G. Aygun G., Ozyuzer L. *Vacuum,* 2015, **120**:8 [Crossref], [Google Scholar], [Publisher]
[17]. Eshaghi A., Graeli A. *Optik* , 2014, **125**: 1478 [Crossref], [Google Scholar], [Publisher]
[18]. Liao W.Y., Chang H., Yang Y.J., Hsu C.C., Cheng I.C., Chen J.Z. *Applied Surface Science*, 2014, **292**:213 [Crossref], [Google Scholar], [Publisher]
[19]. Ko B.C. Wesseling P., Vatamanu O.L., Shiflet G.L., Lewandowski J.J. *Intermetallics*, 2002, **10:**1099 [Crossref], [Google Scholar], [Publisher]
[20]. Khojier K. Savaloni H., Jafari F. *Journal of Theoretical and Applied Physics* , 2002, **7:**1 [Crossref], [Google Scholar], [Publisher]
[21]. Zhao B.X., Zhou J., Rong L.Y. *Transactions of Nonferrous Metals Society of China,* 2010, **20**:1429 [Crossref], [Google Scholar], [Publisher]
[22]. Ahn M.H., Cho E.S., Kwon S.J. *Vacuum*, 2014, **101**:221 [Crossref], [Google Scholar], [Publisher]
[23]. Jeoung H.K., Lee K.M. *Materials Technology,* 2014, **29**:A34 [Crossref], [Google Scholar], [Publisher]
[24]. Moradi-Haji Jafan M., Zamani-Meymian M.R., Rahimi R., Rabbani M. *Microelectronic Engineering,* 2014, **130**:40 [Crossref], [Google Scholar], [Publisher]
[25]. WalshA., Da Silva J., Wei S.H. *Physical Review* 2008, *B* **78**:075211
[Crossref], [Google Scholar], [Publisher]
[26]. Taylor B.N., Kuyatt C. MD: US Department of Commerce Technology Administration *National Institute of Standards and Technology*, 1994. [Google Scholar], [Publisher]
[27]. Ting C.C., Cheng W.L., Lin G.C. *Thin Solid Films,* 2011, **519:**4286 [Crossref], [Google Scholar], [Publisher]

How to cite this manuscript: Mohammad Reza Zamani Meymian*, Mohsen Moradi Haji Jafan, Mahboubeh Rabbani Rabbani, Mahdi Behboudnia. Improving the morphology and electro-optic properties of ITO thin film, by changing argon rate and atmosphere pressure. *Asian Journal of Green Chemistry*, 6(2) 175-184. DOI: 10.22034/ajgc.2022.2.7